Journal of Engineering Science and Technology
Vol. 13, No. 2 (2018) 489 - 504
© School of Engineering, Taylor's University

SORPTION POTENTIAL OF OIL PALM SHELL FOR THE REMOVAL OF CHLORINATED PHENOL FROM AQUEOUS SOLUTION:KINETIC INVESTIGATION

S. M. ANISUZZAMAN[1,*], COLLIN G. JOSEPH[2], DUDUKU KRISHNAIAH[1], W. M. A. W. DAUD[3], E. SUALI [1], F. C. CHEE[2]

[1]Chemical Engineering Programme, Faculty of Engineering,
Universiti Malaysia Sabah, 88400 Kota Kinabalu, Sabah, Malaysia
[2]Water Research Unit, Faculty of Science & Natural Resources,
Universiti Malaysia Sabah, 88400 Kota Kinabalu, Sabah, Malaysia
[3]Department of Chemical Engineering, Faculty of Engineering,
University of Malaya, 50603 Kuala Lumpur, Malaysia.
[*]Correspondence Author: anis_zaman@ums.edu.my

Abstract

In this study, activated carbons (ACs) from oil palm shell (OPS) were prepared using the two-stage self-generated atmosphere method, comprising of a semi-carbonization stage and a chemical activation stage, which were fixed at 300 ^{o}C and 500 ^{o}C respectively. The prepared adsorbents were tested in the removal of 2,4-dichlorophenol (2,4-DCP) from aqueous solution. The samples were impregnated by varying the zinc chloride ($ZnCl_2$) to precursor (OPS) ratio, after which, the final products, ACs, underwent several aspects of chemical and physical characterizations, i.e. percentage of yield, moisture content, ash content, pH, porosity, adsorption kinetics and isotherms (2,4-DCP) and surface chemistry of the adsorbent. The results indicated that the percentage of yield, moisture content and ash content had increased in proportional to the increase in $ZnCl_2$ ratio. It was found that AC4, with the impregnation ration of 1:4 (OPS:$ZnCl_2$) had the highest adsorption capacity of 26.40 mg/g. While the maximum Brunauer, Emmett and Teller (BET) surface area of AC4 was found to be around 1020 m^2/g. Adsorption studies indicated an increased in adsorption capacity in proportional to the increase in adsorbate initial concentration and adsorbent dosage, whereas a higher pH decreased the adsorption capacity. The adsorption isotherm of all the prepared ACs fitted well to the Langmuir model, while the sorption kinetics followed the pseudo-second order, indicating that the adsorption was a single layer chemisorption process.

Keywords: Activated carbon, Two stage self-generated atmosphere; 2,4-dichlorophenol, Oil palm shell.

Nomenclatures	
A_T, K_F K_L, n	Equation constants
B	Constant related to heat of sorption
Co	Concentrations of solution at initial, mg/L)
Ce	Concentrations of solution at equilibrium, mg/L
C	Plot intercept
C_e	Amount of adsorbate in the solution at equilibrium
k_1	Rate constant for pseudo-first-order, min^{-1}
k_2	Rate constant for pseudo-second-order, g/mg min
k_{id}	Rate constant for intraparticle diffusion, mg/g $min^{1/2}$
q_e	Amount of adsorbate adsorbed
q_e	Amount of 2,4-DCP adsorbed per unit mass of the AC at equilibrium
q_t	Amount of 2,4-DCP adsorbed per unit mass of the AC at time
Q_m	Amount of adsorbate adsorbed to form monolayer coverage
R^2	Correlation coefficient
t	Time, min
V	Volume of solution, L
W	Mass of absorbent, g
Abbreviations	
2,4-DCP	2,4-dichlorophenol
AC	Activated carbon
BET	Brunauer, Emmett and Teller
BJH	Barret, Joyner and Halenda
FTIR	Fourier transform infrared spectroscopy
OPS	Oil palm shell
ppb	Parts per billion
SCC	Semi-carbonized carbon
SEM	Scanning electron microscope

1. Introduction

Activated carbon (AC) is a carbonaceous material with extended surface area that renders it the ability for adsorbing chemical contaminants in water or air, depending on its structure [1]. It has been widely used in the decolorization of textile, purification of water, removal of organic pollutants from liquid and gas stream and in the removal of fouled smell and taste from drinking water [2-4]. Pollutants such as chlorinated phenols are considered as major pollutants in the aquatic ecosystem since they are harmful to organisms even at parts per billion (ppb) levels [5]. They can be introduced into the environment through industrial operations such as industrial effluents, paper pulp bleaching process, agricultural runoff, breakdown of chlorophenoxyacetic acid herbicides and water disinfection and deodorization processes with chlorine [6].

Adsorption by AC is the cheapest and fastest way for the removal of water-based pollutants [7-11]. As such, the demand for renewable, abundant and low-cost lignocellulosic materials to be used as precursor for AC is in great demand. One such option is to use Oil palm shell (OPS). In Malaysia, the oil palm milling industry generates large quantities of carbonaceous OPS as by-products which causes disposal and environment problems [12]. Converting OPS into compost is

not recommended due to risk of spreading oil palm related disease to other plantations. OPS has 55.7% of carbon content compared to oil-palm fibers (49.6%), sugar cane bagasse (53.1%) and coffee shells (50.3%) [13]. Therefore OPS is suitable to be used to produce AC with high adsorption ability and as a precursor in the production of AC due to their high carbon content [14]. This will solve the disposal problem and yield a waste to wealth opportunity for other industries.

In this study, OPS as raw material was employed to produce AC through semi-carbonization and chemical activation by using a two-stage self-generated atmosphere method. In the first stage, the precursors was carbonized, then impregnated by activating agent, followed by activation at a fixed time duration [15]. Zinc chloride ($ZnCl_2$) was used as dehydrating and activating agent because it can alter the structure of carbon to form porous structure. $ZnCl_2$ is known as strong dehydrator which subtracts hydrogen and oxygen from raw material during activation process [16]. Impregnation with $ZnCl_2$ causes dehydration which results in charring and aromatization of the carbon skeleton and formation of pore structure. This helps to enhance the adsorption capacity of the carbon produced [17]. Besides that, hydrochloric acid (HCl) generated during the carbonization in the presence of $ZnCl_2$ can reduce the ash content of the carbon obtained. This enables lower temperature to be used to prepared a highly developed microporous AC. In order to study and evaluate the optimal operation condition in producing the best quality of AC, various parameters such as adsorbent dosage and impregnation ratio was manipulated to optimize the prepared carbons. Final products were characterized in several aspects such as yield and ash content. The best AC was chosen to undergo further studies on adsorption isotherm and kinetic

2. Materials and methods

2.1. Preparation of AC

The OPS was obtained from Beaufort Palm Oil Mill in Kampung Batu Tiga, Beaufort, Sabah, Malaysia. Prior to semi-carbonization process, raw material was washed with distilled water several times and subsequently dried in an oven at 110 ^{o}C for 24 hours. This helped to remove any impurities and minimize moisture content [18, 19]. After that, the precursor materials were placed inside a muffle furnace (model Carbolite RHF 1500) and pyrolysed under self-generated atmosphere at 300 ^{o}C for an hour. The semi-carbonized carbon (SCC) was agitated with $ZnCl_2$ aqueous solution of 200 mL at various OPS:$ZnCl_2$ weight ratios ranging from 1:1 to 1:5 and labelled as samples AC1-AC5 [19]. All the OPS were immersed fully into the solutions of $ZnCl_2$ at 85 ^{o}C till the solution completely dried out. The impregnations were carried out in an orbital shaker and subsequently dried at 110 ^{o}C for 24 hours in an oven. Then the samples were activated in a muffle furnace at 500 ^{o}C for 2 hours.

2.2. Washing process

The carbonized sample was washed with 0.01 M HCl solution, at 85 ^{o}C for 30 minutes to eliminate $ZnCl_2$ in excess. Due to the high solubility of $ZnCl_2$ in water, no further washing with water was performed [20]. The pH of each

sample was identified and the samples were dried at 110 ^{o}C for 24 hours to obtain the final product.

2.3. Characterization of AC

Moisture and ash contents were determined according to ASTM D2867-04 and ASTM D2866-94 standards respectively, while the pH was determined according to ASTM D3838 -80 standards. Methods for the determination of the percentage of yield, moisture content, ash content and pH had been described in our previous works [10, 11]. Surface chemistry of the prepared ACs were analyzed using Fourier transform infrared spectroscopy (FTIR) (Thermo Nicolet NEXUS 670) analysis where the spectra's were recorded in the range of 4000-650 cm^{-1}. Scanning electron microscope (SEM) (JEOL JSM-5610LV, Japan) at 10 kV with a different magnification was used to observe the morphological surface of the prepared carbon. The specific surface area and the pore-size distribution were determined using the Brunauer, Emmet and Teller (BET) and Barret, Joyner and Halenda (BJH) methods, respectively. This analysis was done by applying nitrogen gas at 77.3 K using Quanta chrome autosorb automated gas sorption instrument [9].

2.4. Batch equilibrium studies

In this study 2,4-Dichlorophenol (2,4-DCP) was used as the target pollutant. Adsorption experiments were conducted in a batch mode using Erlenmeyer flasks employing several concentrations (5, 10, 15, 20, 25, 30 mg/L). A calibration curve of absorbance versus concentration was constructed using a UV-VIS spectrophotometer data at maximum wavelength of 285 nm. All batch adsorption experiments were replicated three times with the average taken and plotted into graphs. The adsorption capacity at equilibrium, q_e (mg/g) was calculated by using Eq. (1).

$$q_e = \frac{(Co - Ce)V}{W} \quad (1)$$

2.5. Effect of initial concentration on adsorption

600 mL of 2,4-DCP solutions with various initial concentrations (10-40 mg/L) were added to flasks containing 0.5 g of the prepared AC. The mixture was stirred for 3 hours while samples were extracted at given intervals, filtered and analyzed using UV/VIS spectrophotometer.

2.6. Effect of pH on adsorption

The concentration of the target pollutant was fixed at 30 mg/L before 0.5 g of AC was added into the solution. The pH for each solution was adjusted to the required value (3,7 and 9) by adding 5 drops of 0.1 M HCl or 0.1 M NaOH solutions, respectively [21].

2.7. Effect of adsorbent dosage on adsorption

600 mL of 2,4-DCP solution with initial concentration of 30 mg/L was placed in a series of conical flasks with different quantity of adsorbent 0.1, 0.3 and 0.5 g of AC. The mixture was stirred for 3 hours while samples were extracted at given intervals, filtered and analyzed using UV/VIS spectrophotometer [21].

2.8. Adsorption isotherm

Langmuir, Freundlich and Temkin isotherms were applied to obtain the experimental equilibrium isotherm data in order to determine the maximum chlorophenol adsorption capacity of the prepared carbon [22]. The mathematical expressions of these equations can be written as follows [Eqs. (2), (3) and (6)].

Langmuir isotherm, $q_e = \frac{Q_m K_L C_e}{1 + K_L C_e}$ (2)

Freundlich isotherm, $q_e = K_F C_e^{\frac{1}{n}}$ (3)

Temkin isotherm, $q_e = B \ln A_T + B \ln C_e$ (4)

2.9. Adsorption kinetics

In order to determine the kinetics and dynamics of the adsorption of 2,4-DCP onto AC4, pseudo first-order and pseudo second-order were tested. Both of these equations are expressed as follows [Eqs. (5) and (6)] [23].

$$\log(q_e - q_t) = \log(q_e) - \frac{k_1}{2.303} t \quad (5)$$

$$\frac{t}{q_t} = \frac{1}{q_e} t + \frac{1}{k_2 {q_e}^2} \quad (6)$$

2.10. Determination of rate of transport

When one species moves from the solution bulk onto the solid phase, a transport process called intraparticle diffusion takes place. Intraparticle diffusion model was used to determine the rate constant of the transport as follows [Eq. (7)]

$$q_t = k_{id} t^{1/2} + C \quad (7)$$

3. Results and discussion

3.1. Physical characterization

The yield, moisture and ash content percentage along with pH of AC1-AC5 are shown in Table 1.

As shown in Table 1, AC2 with impregnation ratio of $ZnCl_2$ (1:2) had the highest percentage of yield, which was 56.81%. The impregnation ratio of $ZnCl_2$ played an important role in the yield of AC as its increment increased the percentage of yield up to an optimum point. This can be explained by the inhibition of rapid release of volatile organic matter by $ZnCl_2$, thus preventing the

shrinkage of the precursor and resulting in a higher conversion of product from raw material [18]. However, reduction in the percentage of yield occurred after the optimum point due to the degradation of ligonocellulosic matrix from the precursor resulting in increased pore opening which further intensify the dehydration and elimination reactions [24].

Table 1. ACs with their relative yield, moisture, ash and pH.

Sample	Yield (%)	Moisture content (%)	Ash content (%)	pH
AC1	5	2.60	5.00	
AC2	5	3.60	6.42	
AC3	4	4.81	7.33	
AC4	4	5.40	7.62	
AC5	4	6.59	8.02	

The moisture content of ACs showed an increasing trend from AC1 to AC5. Impregnation ratio of $ZnCl_2$ played another big role in this aspect. The moisture content of ACs increased with the impregnation ratios. AC5 had highest moisture content with 6.59% compared to the others. This is due to the increasing dehydration rate of ACs with the impregnation ratios [25]. More hydrogen and oxygen are being subtracted from raw material during the activation process [26].

Ash content of AC increased in proportion to the increased of $ZnCl_2$ ratio. AC5 with $ZnCl_2$ impregnation ratio of (5:1) had the highest ash content with 8.02% as compared to the others. It can be concluded that $ZnCl_2$ is one of the constituents in the ash, thus higher ash content was obtained. High impregnation ratio of $ZnCl_2$ contributes to high ash content due to the formation of a large amount of insoluble inorganic compounds [25].

pH of all the prepared ACs ranged from 5.26 to 6.11. AC1 had the highest pH value of 6.11 while AC5 had the lowest pH value of 5.26. A decreasing trend of pH values was observed regarding to different concentration of $ZnCl_2$. The pH value decreased with higher impregnation ratio of $ZnCl_2$. This can be attributed to the hydrolysis of the metal salt in the presence of natural alkalinity to form acidic metal hydroxides thus reducing the alkalinity of the carbonized shells [25].

3.2. Surface functional group of AC

Figure 1 shows the FTIR spectra for the OPS and the ACs. The spectra for OPS and ACs have three similar spectra at peaks of 1000-1150 cm^{-1}, 1600-1630 cm^{-1} and 3400-3450 cm^{-1}. All the spectra showed a wide adsorption band at 1000-1150 cm^{-1} due to C-O stretching in acid, alcohols, phenols, ethers and esters. There was a sharp and strong peak at 1600-1630 cm^{-1} due to C=C aromatic ring stretching vibration which is enhanced by polar functional group. Another peak shown at approximately 3440 cm^{-1} was attributed to stretching of the O-H hydroxyl groups. An adsorption band at approximately 2910 cm^{-1} which was attributed to the asymmetric and symmetric C-H stretching was found in the spectrum of raw material but not in spectra of ACs. It may due to the strong dehydrating ability of

$ZnCl_2$ to remove a large amount of hydrogen from ACs [27]. Besides that, the peak at 1740 cm^{-1} which was associated with aldehyde and ketone has disappeared in the spectra of ACs. It may due to thermal instability in high temperature, resulting in more weakly bound substituent being removed [18, 19, 28].

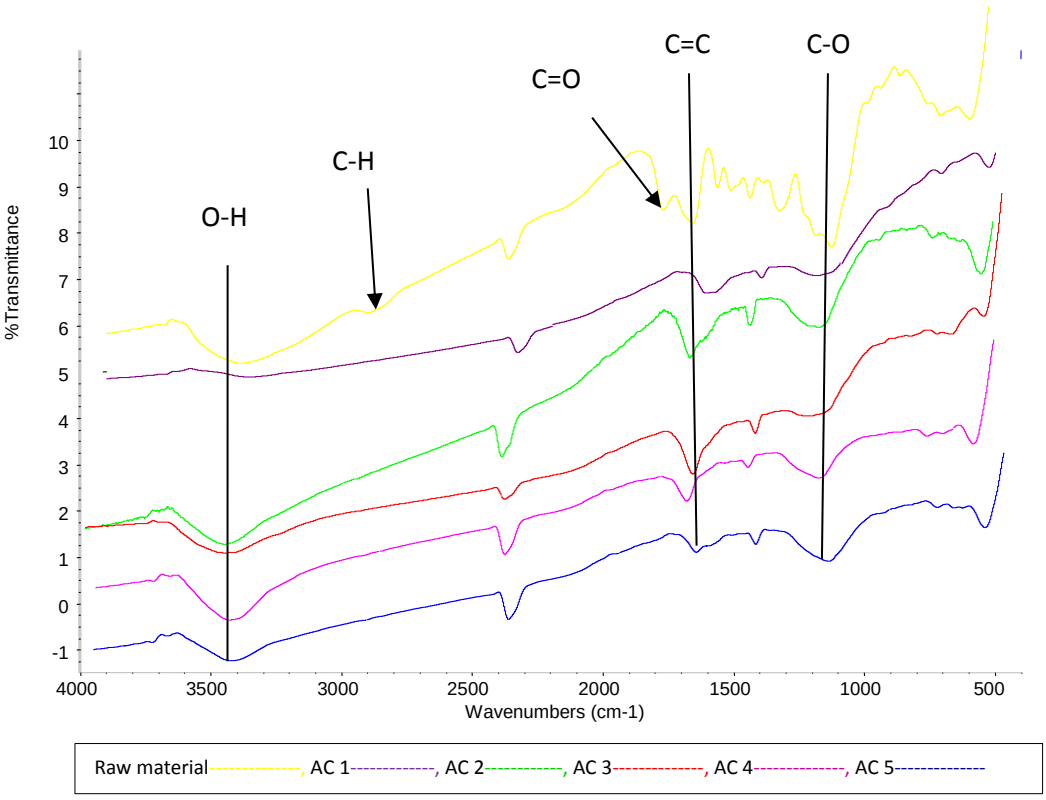

Fig. 1. Combination of spectra for OPS and ACs.

3.3. Morphological study of AC

The SEM was used to identify the porous structure and external surface of the AC. The size and distribution of the pores for the samples were prepared under different conditions as shown in Fig. 2.

Figure 2(a) shows the morphological structure of the OPS, which has a few pores and resin covered pores on its surface. Figure 2(b) and (c) are the micrographs for AC1 and AC2 respectively. AC1 shows tunnel-like structure whereas AC2 shows crystalline structure. AC3 has a lot of impurities clogged on the pores as shown in Fig. 2(d). This may due to the incomplete washing process and $ZnCl_2$ residues left on the surface. AC4 shows a surface of numerous micropores on it. The presence of micropores can have a great effect on the adsorption of 2,4-DCP. This finding concurs with the BET surface area analysis presented in Table 2 and in Fig. 3. While Fig. 2(f) shows a very rough surface and surface damage on AC5. There are only few pores on the surface and this would affect the adsorption adversely.

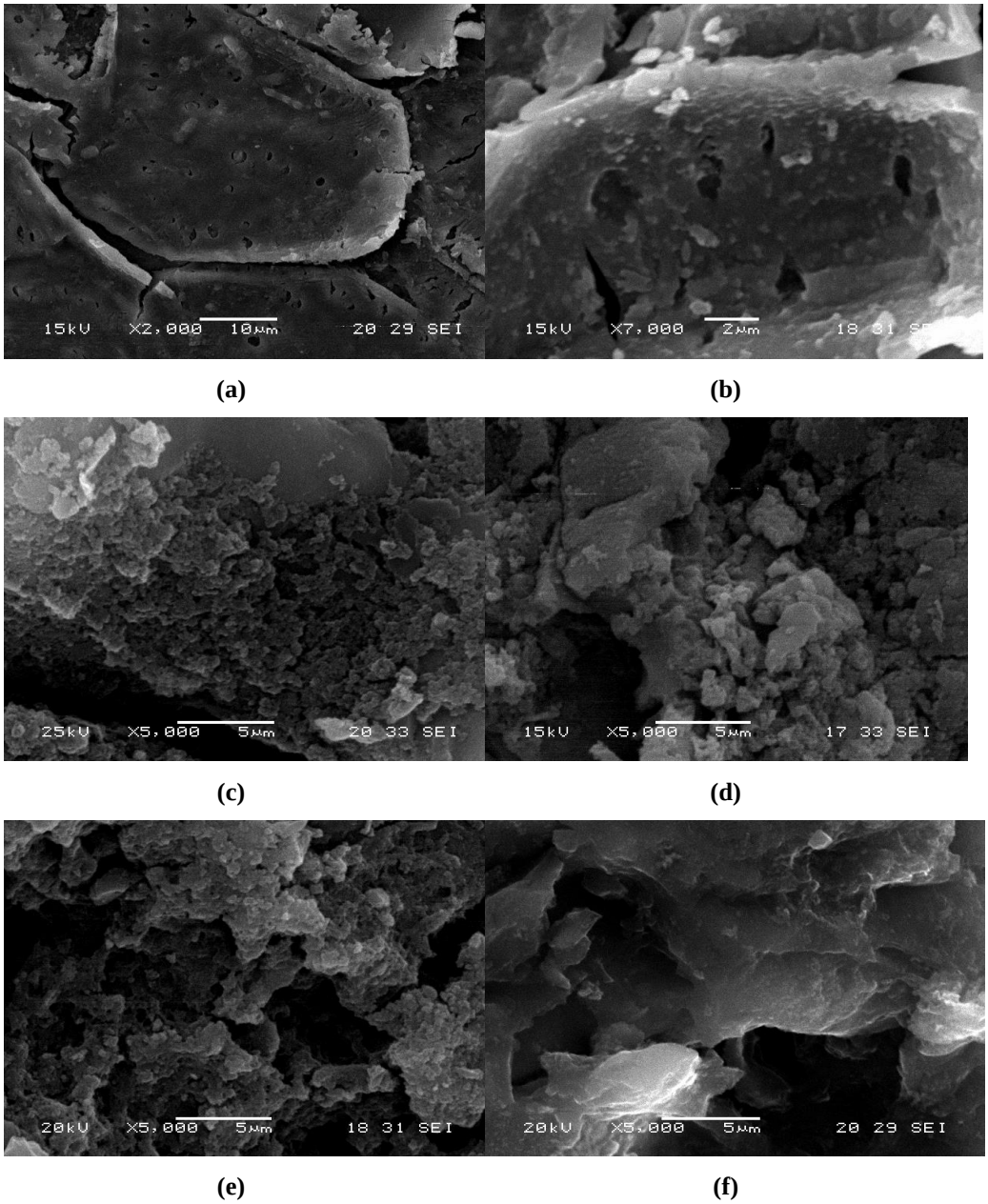

Fig. 2. SEM micrographs of (a) OPS (2000X) (b) AC1 (7000X) (c) AC2 (5000X) (d) AC3 (5000X) (e) AC4 (5000X) (f) AC5 (5000X).

3.4. Specific surface area and pore-distribution

AC4 was selected for surface area and pore distribution analysis. The maximum Langmuir surface area of sample AC4 was found to be 1020 m^2/g and the average pore diameter of 24.4 Å which is comparable with the findings of other

researchers [8-11, 29-31]. Table 2 represents the porous and surface characteristics of AC4.

Table 2. Surface area, pore volume and pore size of AC4.

Surface area	
Langmuir surface area, m^2/g	$1.02x10^3$
BJH method cumulative adsorption surface area, m^2/g	$9.39x10^2$
BJH method cumulative desorption surface area, m^2/g	$9.83x10^2$
Pore volume	
BJH method cumulative adsorption pore volume, m^3/g	$0.38x10^{-2}$
BJH method cumulative desorption pore volume, m^3/g	$0.39x10^{-2}$
Pore size	
Average pore diameter, Å	24.40
BJH method adsorption pore diameter (mode), Å	8.84
BJH method desorption pore diameter (mode), Å	9.15

Figure 3 shows N_2 adsorption-desorption isotherm of AC4 which contains specific information on the porosity of the particles at the temperature of liquid nitrogen.

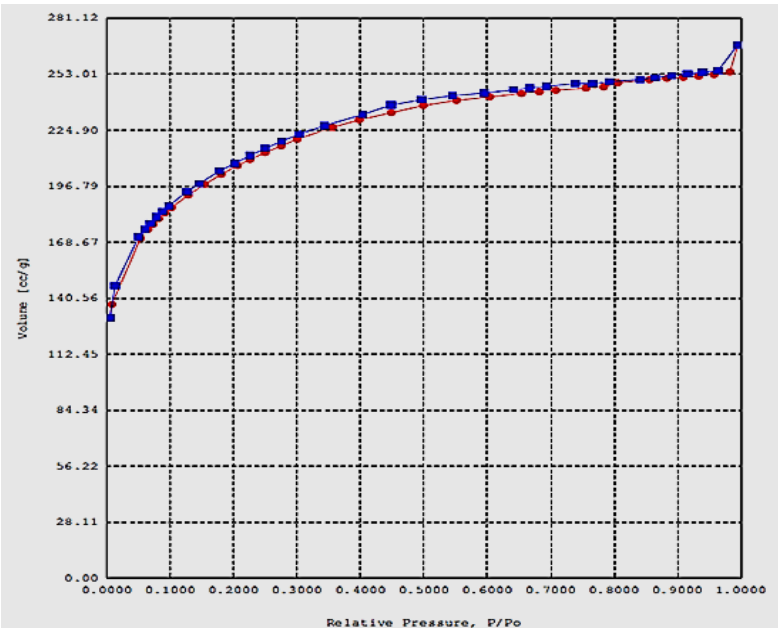

Fig. 3. The N_2 adsorption-desorption isotherms of the AC4.

Figure 3 shows a Type I isotherm with no hysteresis loop. This type of isotherm pattern is called a single-molecule adsorption process and it is characterized by the continuous increase in the adsorption volume until the relative pressure reaches and exceeds a certain value. The isotherm data corroborate with the Langmuir isotherm model in section 3.8, indicating monolayer coverage with chemisorption adsorption properties and is in compliance with the pseudo-second-order reaction kinetics. This is a typical adsorption pattern in microporous solids [9, 10].

3.5. Effect of initial concentration

Figure 4(a) shows that increasing the concentration of the target pollutant resulted in more 2,4-DCP molecules being adsorbed on the 0.5g of AC4 until intial concentration of 30ppm. Afterwhich, the adsorption capacity plateaus. This result is consistent with the findings reported by other researchers [32].

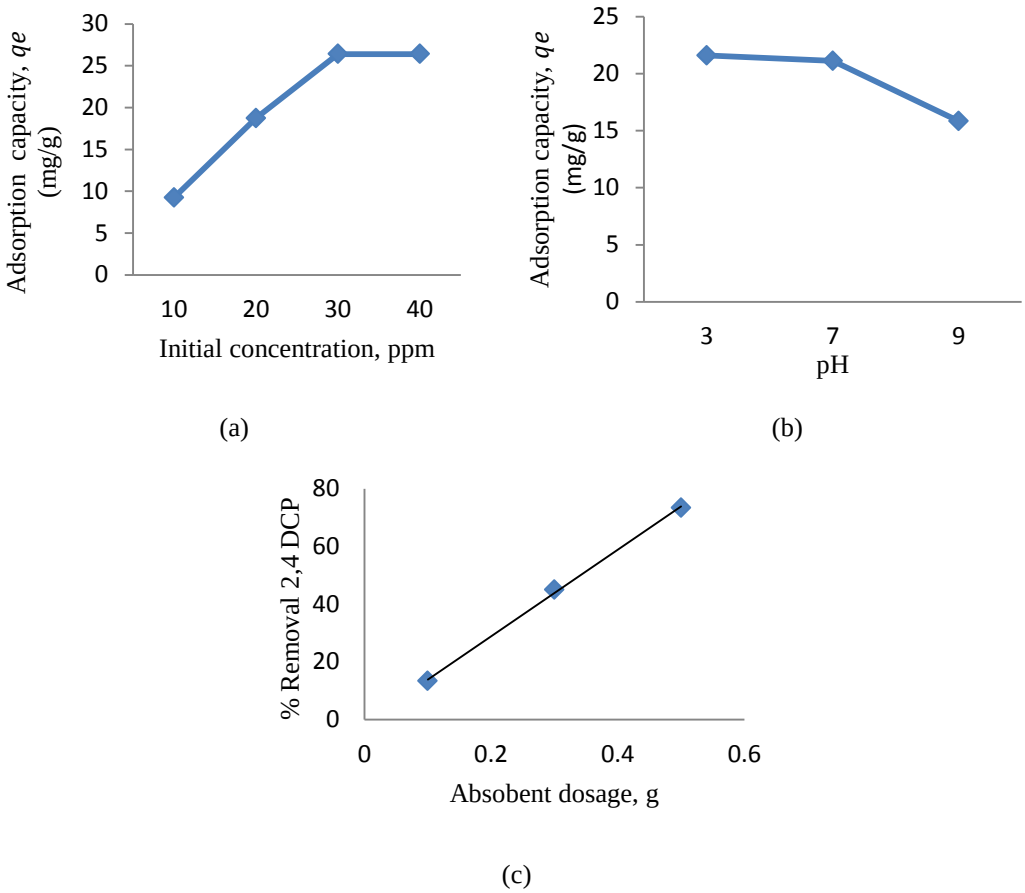

Fig. 4. (a) Effect of initial concentration on the adsorption capacity of AC4 (b) Plot of adsorption capacity against solution pH (c) Effect of adsorbent dosage on 2,4-DCP removal efficiency.

The adsorption uptake at equilibrium, q_e of AC4 increased from 8.04 to 26.40 mg/g as the initial concnetration of 2,4-DCP increased from 10 to 30 ppm. It can be explained by a large amount of vacant pores on the surface of activated carbon at the beginning of adsorption [33]. An increasing concentration gradient between adsorbate in solution and adsorbate in the adsorbent exists [34]. As the concentration increases, more adsorbate molecules are uptaked by the pores until they achieve equilibrium in which no more vacant pores for adsorption. At 40 ppm concentration of 2,4-DCP, the adsorption uptake of AC remains the same, it

is due to all pore sites are being occupied and no more spaces for the remaining of adsorbates to adsorb onto, resulting in an equilibrium is achieved.

3.6. Effect of pH

The pH of the adsorption medium plays an important role in adsorption of 2,4-DCP by AC [35]. The effect of pH on adsorption of 2,4-DCP was studied over a pH range of 3–9 with the initial concentration of 2,4-DCP fixed at 30 mg/L. Figure 4(b) shows the adsorption capacity of AC decreases with higher pH. Acidic medium with pH 3 had the highest adsorption uptake value of 21.60 mg/g whereas lowest uptake recorded was at pH 9 with 15.84 mg/g. It is attributed to the 2,4-DCP, which is either neutral or positively charged in lower pH [36]. At acidic medium, 2,4-DCP mostly exists as neutral species and the adsorbent surface is positively charged. There is no electrostatic repulsion between the adsorbent and adsorbate. Therefore, a strong attraction exists between the adsorbate and absorbent. At pH value of 9, the phenol group of the 2,4-DCP dissociates and forms phenolate anion while the surface functional groups on AC is either neutral or negatively charged [36]. Electrostatic repulsion between the same charges of adsorbent and adsorbate reduces the adsorption capacity. Similar observation was reported by researchers working with rice husk [37].

3.7. Effect of adsorbent dosage

The effect of adsorbent dosage on the adsorption of 2,4-DCP can be concluded from Figure 4(c). The maximum adsorption of 2,4-DCP obtained with 0.5 g of AC4 was 73.33%. It can be explained by the number of available pore sites for adsorption increase with adsorbent dosage. More adsorbate molecules adsorb onto the carbon surface, resulting in a higher percentage of 2,4-DCP removal.

3.8. Adsorption isotherms

The plot for Langmuir, Freundlich and Temkin are shown in Fig. 5 whereas the data is shown in Table 3.

Table 3 .Langmuir, Freundlich and Temkin adsorption isotherm for adsorption of 2,4 DCP by AC4.

Sample	Langmuir model			Freundlich model			Temkin model		
	K_L	Q_m	R^2	K_F	n	R^2	A_T	B	R^2
AC4	0.2358	33.78	0.9438	102.78	1.994	0.7875	1.741	8.4991	0.8348

The correlation coefficient (R^2) values of the isotherm models were used to ascertain which one fits the adsorption data of AC4. According to the data shown in Table 3, Langmuir model had a better correlation coefficient value, R^2 of 0.9438. This proved that the surface of AC is flat with no corrugations on it and single-layered adsorption occurred on the adsorbing sites of AC4 [29, 30].

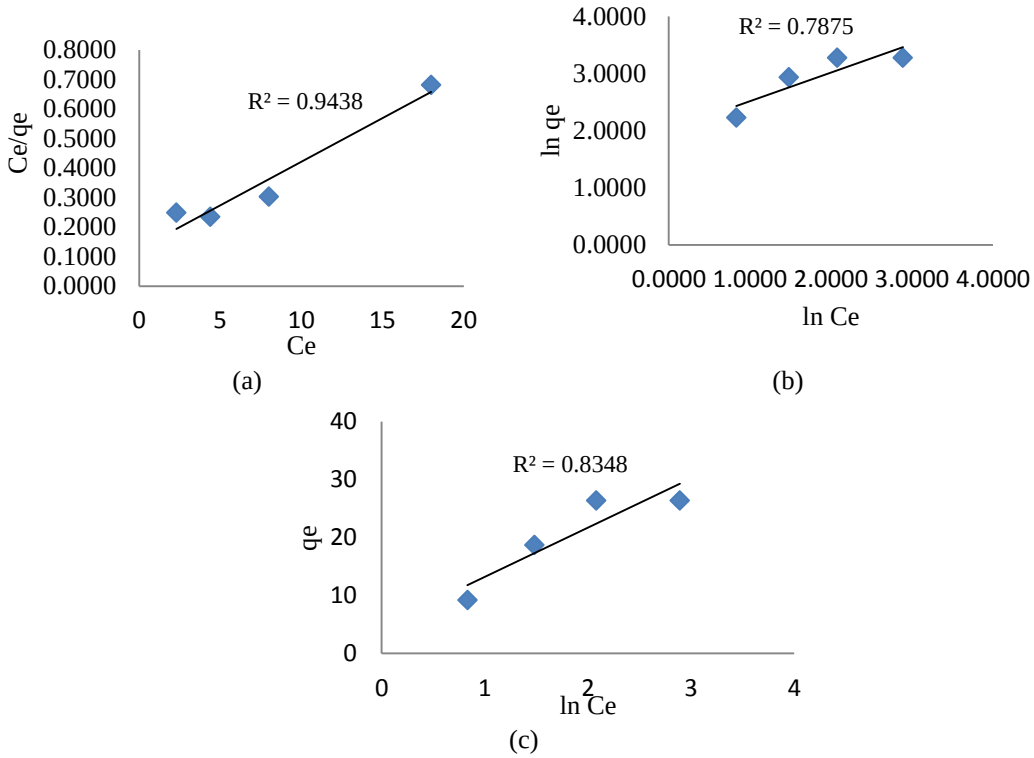

Fig. 5. Plot for the adsorption of 2,4-DCP by AC4
(a) Langmuir isotherm (b) Freundlich isotherm (c) Temkin isotherm.

3.9. Adsorption kinetics

In order to determine the kinetics and dynamic of adsorption of 2,4-DCP on the AC4, pseudo first-order and pseudo second-order were used. Figures 6(a) and (b) show the linear graph of $\log(q_e - q_t)$ against t for pseudo first-order and $\frac{t}{q_t}$ versus t which was constructed for pseudo second-order respectively. Pseudo second-order had a higher correlation coefficient value of 0.9125. It showed that the kinetics and dynamic of adsorption of 2,4-DCP for AC4 fitted well into pseudo second-order. In this model, the rate-determining step is the surface adsorption that is in conformity with chemisorption, where the removal of 2,4-DCP from its solution was attributed to physicochemical interaction between adsorbate and absorbent [38].

3.10. Determination of rate of transport

The transport mechanism was determined by plotting the amount of adsorbed species against a function of retention time. Correlation coefficient and their relationship were investigated. Figure 7 shows that the plot is a linear step, corresponding to the fast uptake of adsorbate and the equation was found to be as below [Eq. (8)].

$$q_t = 2.0797t^{1/2} - 1.0965 \quad (8)$$

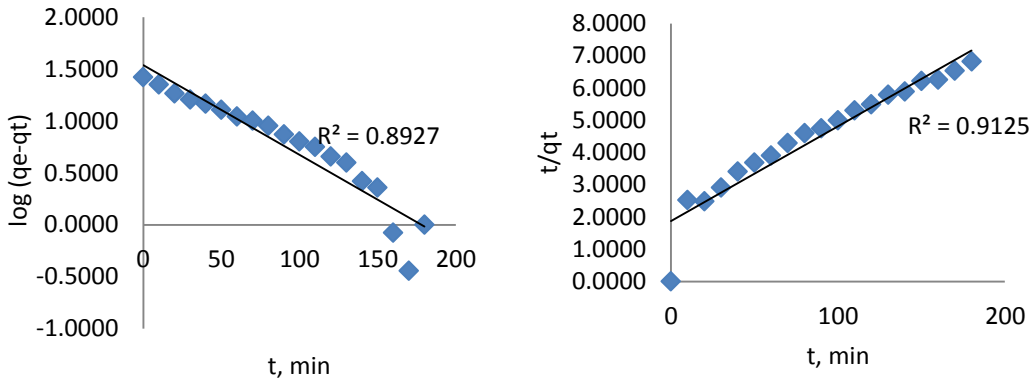

(a) (b)

Fig. 6. Plot for the adsorption of 2,4-DCP by AC4
(a) Pseudo first-order (b) Pseudo second-order.

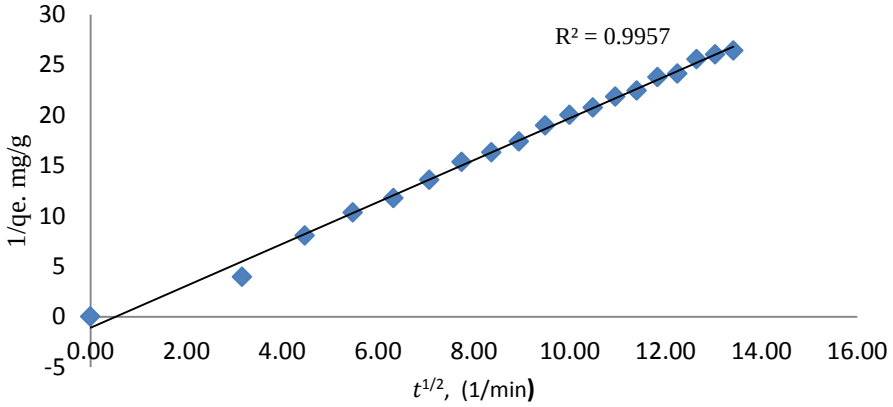

Fig. 7. Plot of adsorption capacity against $t^{1/2}$.

The transport of 2,4-DCP onto OPS based ACs was only controlled by chemisoprtion process, as it has a straight line passing through the origin and a negative value of intercept C_i. The deviation of the line from origin indicates that the rate-limiting step is not only affected by intrapartice transport, but affected by the transport of adsorbate through the particle-sample interphase on the pores as well as the availablility of pores on the surface of the adsorbent [38].

4. Conclusions

In this study, $ZnCl_2$ was used to chemically activate OPS and produce ACs to be used for the removal of 2,4-DCP from aqueous medium. AC4 was the best AC, which had the highest adsorption capacity. Its adsorption capacity decreased with higher pH due to the strong repulsion forces between adsorbate and adsorbent surface. Adsorbent dosage had an significant effect on the adsorption as higher

dosage would remove more 2,4-DCP from the aqueous medium. The maximum BET surface area of AC4 was found to be around 1020 m^2/g. Adsorption equilibrium of AC4 was best described by Langmuir isotherm equation with maximum monolayer adsorption capacity of 26.40 mg/g for the removal of 2,4-DCP from aqueous medium. Besides, Pseudo second-order was found to describe the adsorption kinetic best and was in collaboration with BET surface area and adsorption isotherms, proving that the chemisorption was the dominant rate-determining step in this adsorption study.

Acknowledgement

This research was supported by the Research Management Center of Universiti Malaya in collaboration with the Center of Research and Innovation of Universiti Malaysia Sabah (Grant No. GL0111 or UM Project code: CG071-2013). These contributions are gratefully acknowledged.

References

1. Karen, J.S.; Greisly, D.M.; and Puello, J. (2014). Adsorption of chromium (VI) by activated carbon produced from oil palm endocarp. *Chemical Engineering Transactions*, 37, 721-726.
2. Barton, S.S. (1987). The adsorption of methylene blue by activated carbon. *Carbon*, 25(3), 343-350.
3. Cheremisnoff, P.N.; and Morresi, A.C. (1978). Carbon Adsorption Applications. *Ann Arbor Science Publishers*, Inc, Michigan, 1-5.
4. Chmiola, J.; Yushin, G.; Gogotsi, Y.; Portet, C.; Simon, P.; and Taberna, I. (2006). Anomalous increase in carbon capacitance at pore sizes less than 1 nm. *Science*, 313, 1760-1763.
5. Chapman, P.M.; Romberg, G.P.; and Vigers, C.A. (1982). Design of monitoring studes for priority pollutants. *Journal Water Pollution Control Federation*, 54(3)**,** 292-297.
6. Exon, J.H. (1984). A review of chlorinated phenols. *Journal Veterinary and Human Toxicology*, 26(6), 508-520.
7. Podkoscielny, P.; and Marijuk, A. D. (2003). Heterogeneity of Active Carbons in Adsorption of Phenol Aqueous Solutions. *Applied Surface Science***,** 205(1-4), 297-303.
8. Joseph, C.G.; Bono, A.; Anisuzzaman, S.M.; and Krishnaiah, D. (2014). Application of soot in the removal of 2, 5-Dichlorophenol in aqueous medium. *Journal of Applied Sciences*, 1 (23), 3182-3191.
9. Anisuzzaman, S.M.; Joseph, C.G.; Taufiq-Yap, Y.H.; Krishnaiah, D.; and Tay, V.V. (2015). Modification of commercial activated carbon for the removal of 2,4-dichlorophenol from simulated wastewater. *Journal of King Saud University- Sciences*, 27(4), 318-330.
10. Anisuzzaman, S.M.; Joseph, C.G.; Daud, W.M.A.W.; Krishnaiah, D.; and Yee, H.S. (2015). Preparation and characterization of activated carbon from *Typha orientalis* leaves. *International Journal of Industrial Chemistry*, 6(1), 9-21.
11. Anisuzzaman, S.M.; Joseph, C.G.; Krishnaiah, D.; Bono, A.; and Ooi, L.C. (2015). Parametric and adsorption kinetic studies of methylene blue removal

from textile simulated sample using Durian (*Durio zibethinus Murray*) skin. *Water Science and Technology*, 72(6), 896-907.

12. Allwar, A.M.N.; Bin Md Noor and Nawi M.A.M. (2008). Textural characteristics of activated carbons prepared from oil palm shells activated with $ZnCl_2$ and Pyrolysis Under Nitrogen and Carbon Dioxide. *Journal of Physical Science*, 19(2), 93-104.
13. Rincon, S.L.; and Gomez, A. (2012). Comparative behaviour of agricultural biomass residues during thermochemical processing. *Global NEST Journal*, 14(2), 111-117.
14. Tan, J. S.; and Ani, F. N. (2004). Carbon molecular sieve produced from oil palm shell for air separation. *Separation and Purification Technology*, 35(1), 47-54.
15. Joseph, C.G. and Yii, F. (2008). Textural and chemical characterisation of activated carbon prepared from rice husk (oryza sativa) using a two-stage activation process. *Journal of Engineering Science and Technology*, 3(3), 234-242.
16. Kim, J.W.; Sohn, M.H.; Kim, D.S.; Sohn, S.M.; and Kwon, Y.S. (2001). Production of granular activated carbon from waste walnut shell and its adsorption characteristics for Cu^{2+} ion. *Journal of Hazardous Materials*, 85(3), 301-315.
17. Caturla, F.; Molina-Sabio, M.; and Rodriguez-Reinoso, F. (1991). Preparation of activated carbon by chemcal activation with $ZnCl_2$. *Carbon*, 29(7), 999-1007.
18. Guo, J.; and Lua, A.C. (2000) Preparation and characterization of adsorbents from oil palm fruit solid wastes. *Journal of Oil Palm Research*, 12, 64-70
19. Guo, J.; and Lua, A.C. (2002). Characterization of adsorbent prepared from oil-palm shell by CO_2 activation for removal of gaseous pollutants. *Materials Letters*, 55(5), 334-339.
20. Gañán-Gómez, J.; Macías-García, A.; Díaz-Díez, M.A.; González-García C.; and Sabio-Rey, E. (2006). Preparation and characterization of activated carbons from impregnation pitch by $ZnCl_2$. *Applied Surface Science*, 252(17), 5976-5979.
21. Ekpete, O.A.; Horsfall M.J. and Spiff, A.I. (2012). Removal of chlorophenol from aqueous solution using fluted pumkin and commercial activated carbon. *Asian Journal of Natural and Applied Sciences*, 1(1), 96-105.
22. Ahmed M.J.; and Theydan, S.K. (2013). Adsorption of p-chlorophenol onto microporous activated carbon from Albizia lebbeckseed pods by one-step microwave-assisted activation. *Journal of Analytical and Applied Pyrolysis*, 100, 253-260.
23. Wang, S. B.; Zhu, Z.H.; Anthony, C.; Haghseresht, F.; and Lu, G.Q. (2005). The physical and surface chemical characteristics of activated carbon and the adsorption of methylene blue from wastewater. *Journal of Colloid and Interface Science*, 284, 440-446.
24. Bouchemal, N.; Belhachemi, M.; Merzougui, Z.; and Addoun, F. (2009). The effect of temperature and impregnation ratio on the active carbon porosity. *Desalination and Water Treatment*, 10 (1-3), 115-120.

25. Owabor, C.N.; and Iyaomolere, A.I. (2013). Evaluation of the influence of salt treatment on the structure of pyrolyzed periwinkle shell. *Journal of Applied Sciences and Environmental Management*, 17, 321-327.
26. Mohammad, K.A. and Ansari, R. (2009). Activated charcoal: preparation, characterization and applications: A review article. *International Journal of Chem Tech Research*, 1 (4), 859-864.
27. Jagtoyen, M.; and Derbyshire, F. (1998). Activated carbons from yellow poplar and white oak by H_3PO_4 activation. *Carbon*, 36(7), 1085-1097.
28. Guo, J.; and Lua, A.C. (2003). Surface Functional Groups on Oil-Palm-Shell Adsorbents Prepared by H_3PO_4 and KOH Activation and their Effects on Adsorptive Capacity. *Chemical Engineering Research and Design*, 81(5), 585-590.
29. Hameed, B.H.; Tan, I.A.W.; and Ahmad, A.L. (2008). Adsorption isotherm, kinetic modeling and mechanism of 2,4,6-trichlorphenol on coconut husk based activated carbon. *Chemical Engineering Journal*, 144(2), 235-244.
30. Hameed, B.H. (2009). Evaluation of papaya seeds as a novel non-conventional low-cost adsorbent for removal of methylene blue. *Jounal of Hazardous Materials*, 162(2-3), 939-944.
31. Krishnaiah, D.; Anisuzzaman, S.M.; Bono, A. and Sarbatly, R. (2013). Adsorption of 2,4,6-trichlorophenol (TCP) onto activated carbon. *Journal of King Saud University - Science*, 25**(**3), 251-255.
32. Shaarani, F.W.; and Hameed, B.H. (2010). Batch adsorption of 2,4-dihlorophenol onto activated carbon derived from agricultural waste. *Desalination*, 255 (1-3), 159-164.
33. Hamad, B.K.; Noor, A.M.; and Rahim, A.A. (2011). Removal of 4-Chloro-2-Methoxyphenol from aqueous solution by adsorption to oil palm shell activated carbon activated with K_2CO_3. *Journal of Physical Science*, 22(1), 39-55.
34. Sathishkumar, M.; Binupriya, A.; Kavitha, R. D.; and Yun, S.E. (2007). Kinetic and isothermal studies on liquid-phase adsorption of 2,4-dichlorophenol by palm pith carbon. *Bioresource Technology*, 98(4), 866-873.
35. Aksu, Z.; and Yener, J. (2001). A comparative adsorption/biosorption study of mono chlorinated phenols onto various sorbents, *Waste Management*, 21(8**)**, 695-702.
36. Sathishkumar, M.; Binupriya, A.; Kavitha, R.D.; Selvakumar, S.; Jayabalan, R.; Choi, J.G.; and Yun, S.E. (2009). Adsorption potential of maize cob carbon for 2,4dichlorophenol removal from aqueous solutions: Equilibrium, kinetics and thermodynamics modeling, *Chemical Engineering Journal*, 147(2-3), 265-271.
37. Mubeena, A.; Bhanger, M.J.; Shahid, I.; and Hasany, S.M. (2006). Sorption potential of rice husk for the removal of 2,4-dichlorophenol from aqueous solution:Kinetic and thermodynamic investigation. *Jounal of Hazardous Materials*, 128(1), 44-52.
38. Badmus, M.A.O.; Audu, T.O.; and Anyata, B.U. (2007) Removal of lead ion from industrial wastewaters by activated carbon prepared from periwinkle shells (*Typanotonus fuscatus*). *Turkish Journal of Engineering and Environmental Science*, 31, 251-263.